Trends and Variability of North American Cool-Season Extratropical Cyclones: 1979–2019

ROBERT FRITZEN,[a] VICTORIA LANG,[b] AND VITTORIO A. GENSINI[a]

[a] *Department of Geographic and Atmospheric Sciences, Northern Illinois University, DeKalb, Illinois*
[b] *Department of Atmospheric Science, University of Wisconsin–Milwaukee, Milwaukee, Wisconsin*

(Manuscript received 9 December 2020, in final form 15 July 2021)

ABSTRACT: Extratropical cyclones are the primary driver of sensible weather conditions across the midlatitudes of North America, often generating various types of precipitation, gusty nonconvective winds, and severe convective storms throughout portions of the annual cycle. Given ongoing modifications of the zonal atmospheric thermal gradient resulting from anthropogenic forcing, analyzing the historical characteristics of these systems presents an important research question. Using the North American Regional Reanalysis, boreal cool-season (October–April) extratropical cyclones for the period 1979–2019 were identified, tracked, and classified on the basis of their genesis location. In addition, bomb cyclones—extratropical cyclones that recorded a latitude-normalized pressure fall of 24 hPa in 24 h—were identified and stratified for additional analysis. Cyclone life span across the domain exhibits a log-linear relationship, with 99% of all cyclones tracked lasting less than 8 days. On average, ≈270 cyclones were tracked across the analysis domain per year, with an average of ≈18 yr^{-1} being classified as bomb cyclones. The average number of cyclones in the analysis domain has decreased in the last 20 years from 290 per year during 1979–99 to 250 per year during 2000–19. Decreasing trends in the frequency of cyclone track counts were noted across a majority of the analysis domain, with the most significant decreases found in Canada's Northwest Territories, Colorado, and east of the Graah Mountain Range. No significant interannual or spatial trends were noted in the frequency of bomb cyclones.

KEYWORDS: Extratropical cyclones; Synoptic climatology; Climate variability

1. Introduction and background

Extratropical cyclones (ETCs) are responsible for various meteorological phenomena and natural hazards, ranging from severe convective storms and significant rainfall to heavy snow, gusty winds, and extreme temperatures (Salmon and Smith 1980; Uccellini et al. 1984; Fink et al. 2009; Lackmann 2011; Bentley et al. 2019). Forming through tropospheric disturbances in the wave pattern at the mid- and upper levels of the atmosphere, ETCs are a vital driver of poleward thermal and moisture transport (Chang et al. 2002), and as a result, are critical when analyzing Earth's climate system (Holton 2004; Lackmann 2011; Martin 2013). The most notable of these systems form through sustained advection of differential cyclonic potential vorticity, the absolute cyclonic rotation of an air parcel bounded between two isentropic surfaces (Holton 2004; Lackmann 2011; Martin 2013). ETCs are inherently dynamic and have a varied range of intensity, longevity, frequency, and three-dimensional structure. Given their importance in the global budget of energy transport, spatiotemporal climatologies (e.g., average number of cyclones, mean cyclone track, interannual variability of frequency) of ETCs provide an important statistical metric to assess the behavior of Earth's weather and climate.

Frequency and spatial origin of ETC genesis has been explored in numerous studies over the years (e.g., Reitan 1979; Ulbrich et al. 2009; Wang et al. 2013; Vose et al. 2014; Colle et al. 2015; Befort et al. 2016). For example, a sample of 146 Canadian ETCs identified three favored locations leeward of the Canadian Rockies for cyclogenesis: 1) southwest Alberta Range, 2) MacKenzie Mountains, and 3) northern British Columbia Range. The spatial frequency maxima appeared 200–250 km from the Continental Divide with a documented lag between cyclogenesis and peak intensification (Chung and Reinelt 1973; Chung et al. 1976). Across a broader North American domain, a study examining ETCs from 1958 to 1977 found the most active areas for cyclogenesis along the eastern contiguous United States (CONUS), Gulf of Mexico (especially in boreal winter), eastern Colorado, portions of the Great Basin, and lee of the Rocky Mountains of Alberta extending into the Northwest Territories (Whittaker and Horn 1981). This analysis also observed a downward trend in cyclogenesis frequency across Alberta, the Northwest Territories, a slight (but variable) decline across the East Coast, and no trend in Colorado. Although a decline of North American ETC frequency was noted, an analysis of the Northern Hemisphere midlatitude climatology revealed no trend. In addition, a maximum frequency of ETCs was found in March, with a minimum found in September (Whittaker and Horn 1981).

In extreme cases of ETC genesis, the central surface pressure of an ETC can exhibit a latitudinal-normalized decrease of 24 hPa or more in a 24-h period. This minimum decrease of 24 h is defined at 60°N as a unit of 1 Bergeron (B; $1\,B = 24\sin\phi/\sin60°$), where ϕ is latitude and the constant 24 has units of hectopascals per day. Values meeting or exceeding 1 B are commonly referred to as explosive cyclogenesis and/or bomb cyclones (Sanders and Gyakum 1980; Roebber 1984; Gyakum et al. 1989; Chen et al. 1992). Explosive cyclogenesis can be a challenge to forecast and, depending on location, can cause significant societal impacts (Uccellini et al. 1984; Yiou and Nogaj 2004; Ulbrich et al. 2009). Characteristics of bomb cyclones have been analyzed between

Corresponding author: Robert Fritzen, rfritzen1@niu.edu

DOI: 10.1175/JAMC-D-20-0276.1

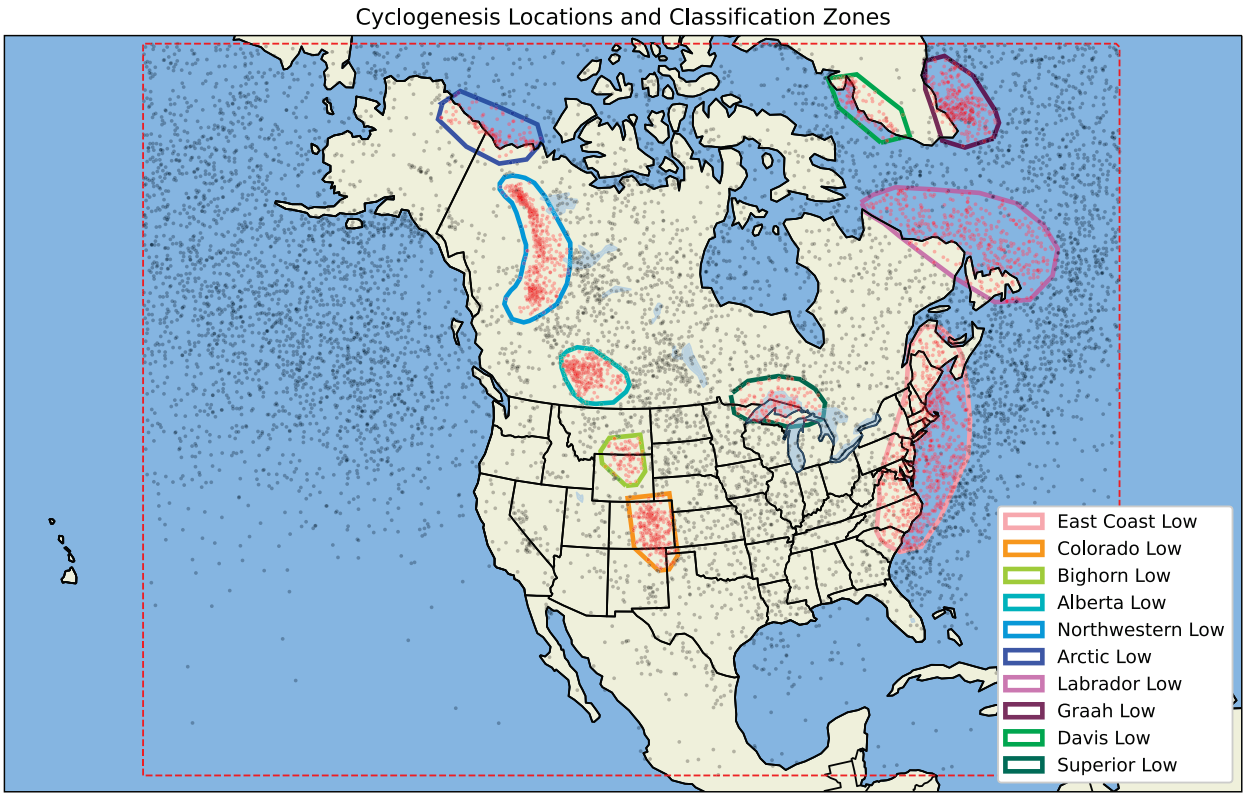

FIG. 1. The 10 cyclogenesis-region classifications used in this study. Red and black dots indicate classified and unclassified extratropical cyclones, respectively. The dashed red bounding box denotes the analysis domain.

1979 and 2008 using ERA-Interim data for both the Northern and Southern Hemispheres, finding that bomb cyclones tend to be faster, deeper, and longer lived relative to nonbomb cyclones (Reale et al. 2019). Although bomb cyclones can occur over land, rapid deepening often occurs along coastlines as a result of favorable baroclinic and diabatic processes that are typically important for their evolution (Tracton 1973; Sanders and Gyakum 1980; Roebber 1984; Reed et al. 1988; Bullock and Gyakum 1993; Gyakum and Danielson 2000; Roebber and Schumann 2011). Climatological analyses of explosive cyclogenesis have tied the frequency of explosive cyclones to that of the interannual occurrence of all ETCs, but with little statistical significance or variations in the running mean of bomb cyclones (Allen et al. 2010).

Several climatological analyses have demonstrated that a 30-yr window is desired for the optimal calculation of atmospheric trends and variability (WMO 1971; Lamb and Changnon 1981; WMO 1989; Pnevmatikos and Katsoulis 2006). Of the studies that considered a time period of 30 or more years, ETC tracks in the Northern Hemisphere have been shifting poleward and increasing in intensity (Wang et al. 2006; Karl et al. 2009; McDonald 2011; Wang et al. 2013; Vose et al. 2014; Tamarin and Kaspi 2017). Some studies have attributed this poleward shift in ETC tracks as a decreasing trend in ETC counts for the midlatitudes with a subsequent increase in high-latitude ETC counts in the Northern Hemisphere (McCabe et al. 2001; Karl et al. 2009; Vose et al. 2014). Although a couple of these studies reported an increase in high-latitude ETC frequency, there is a significant amount of research that suggests a decreasing trend for ETCs across the Northern Hemisphere, particularly in both the mid- and high-latitude regions (Sickmöller et al. 2000; Gulev et al. 2001; McCabe et al. 2001; Wang et al. 2006; Raible et al. 2008; Ulbrich et al. 2009). One such study that considered multiple reanalyses with different spatiotemporal resolutions found conflicting conclusions in the trends of ETC frequency, which perhaps highlights the importance of data quality and resolution in space and time (Befort et al. 2016). In addition, large scale teleconnections such as El Niño–Southern Oscillation, the North Atlantic Oscillation, the Madden–Julian oscillation, the Arctic Oscillation, and the quasi-biennial oscillation have been demonstrated to influence the interannual frequency, intensity, and mean track of ETCs (Hirsch et al. 2001; Eichler and Higgins 2006; Wang et al. 2011; Bernhardt and DeGaetano 2012; Grise et al. 2013; Attard and Lang 2019).

This study seeks to explore the spatial distribution, frequency, and intensity of ETCs over the 40-yr period 1979–2019. This study is unique to previous work as it is accomplished using a relatively high resolution regional reanalysis (≈32-km horizontal grid spacing; 3 hourly). The higher resolution of data mitigates an important caveat associated with previous studies using coarser resolution global reanalysis data, where cyclone counts have been found to be underestimated by 5%–15% (Zolina and Gulev 2002). Additionally, the higher resolution regional reanalysis allows for more in-depth spatial statistics,

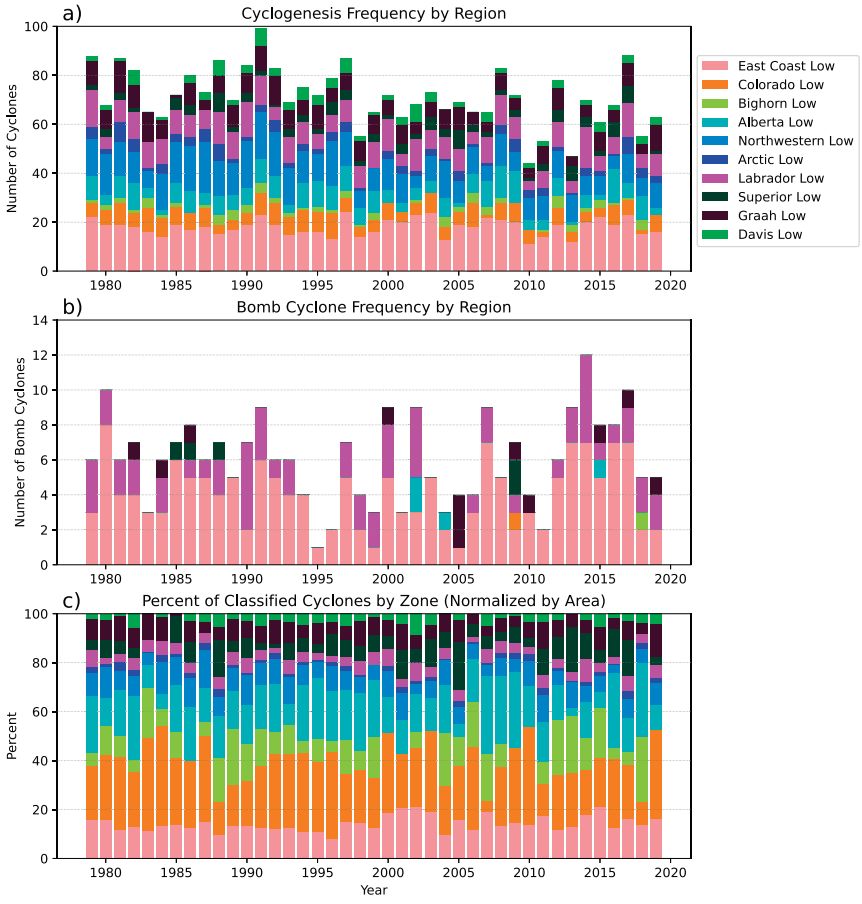

FIG. 2. Annual frequency of (a) all cyclones and (b) bomb cyclones by genesis classification region for the period 1979–2019. Also shown are (c) the area-normalized cyclone totals by region shown as a percent of the classified total.

adding detailed context to overarching findings from the larger body of literature. Section 2 describes the selected data, the cyclone tracking procedure, and classification routines. Section 3 presents various aspects of the North American ETC climatology, including statistical findings, and specific analyses of explosive cyclogenesis. Sections 4 and 5 provide a discussion of results and conclusions from the results, respectively.

2. Data and methods

a. Reanalysis data

This study uses the National Centers for Environmental Prediction (NCEP) North America Regional Reanalysis (NARR) dataset (Mesinger et al. 2006). NARR has a horizontal grid spacing of ~32 km, 29 vertical pressure levels, and a temporal interval of 3 h. Studies that have tracked mean sea level pressure (MSLP) features using NARR, such as tropical cyclones, found a suitable level of accuracy with only minor location errors and more accurate representation of vertical features when compared with global reanalyses such as the 0.5° CFSR (Zick and Matyas 2015).

ETCs are most frequently observed across North America during boreal winter and secondarily in the transition seasons (Sanders and Gyakum 1980; Roebber 1984; Changnon et al. 1995). With this consideration, this study examines NARR data from October to April for the 40-yr study period 1979–2019. While the domain of NARR extends beyond the analysis window used in this study (Fig. 1), the region outside the analysis window was excluded to prevent any cyclone that formed outside the NARR domain and then moved into it from being erroneously tallied as genesis of a new ETC. This excluded region constitutes a 30-gridpoint buffer around the edges of the native NARR domain.

b. Cyclone tracking

Throughout the last several decades, innumerable algorithms using a variety of atmospheric variables have been utilized to track and study ETC tendencies (Sinclair 1994; Hodges 1996; Hoskins and Hodges 2002). In particular, algorithms using MSLP have been shown to be an effective and efficient way to automate the tracking and cataloging of such cyclones (Alpert et al. 1990; Le Treut and Kalnay 1990; Murray and Simmonds 1991; König et al. 1993; Hodges 1994; Sinclair 1994; Sinclair and Watterson 1999; Blender and Schubert 2000). This study adapts the eddy tracking algorithm from Chelton et al. (2011), which used sea surface height to analyze mesoscale variability of the global ocean. Herein, NARR mean sea level

TABLE 1. Summary statistics of all cyclone classifications, including total cyclones, minimum and maximum, average, standard deviation, and a linear regression of cyclone frequency over the 40-year analysis window (statistically significant trends are shown in boldface text).

Classification	Total cyclones	Min (yr)	Max (yr)	Avg	Std dev	Linear regression slope (p value)
East Coast	741	11 (2010)	24 (1997)	18.073	3.367	0.003 (<0.945)
Colorado	258	1 (2007)	11 (1996)	6.293	2.266	**−0.065 (0.03)**
Bighorn	80	0 (1986)	5 (2012)	1.951	1.413	−0.002 (<0.935)
Alberta	292	1 (2013)	14 (2016)	7.122	3.322	−0.024 (0.589)
Northwest	500	5 (2002)	21 (1987)	12.195	4.098	**−0.216 (<0.001)**
Arctic	128	0 (1999)	8 (1981)	3.122	1.770	−0.036 (0.133)
Labrador	384	4 (2010)	17 (2014)	9.366	3.058	−0.045 (0.277)
Graah	302	1 (1985)	13 (1981)	7.366	2.526	**−0.071 (0.033)**
Davis	113	0 (1983)	7 (1991)	2.756	1.832	−0.011 (0.665)
Superior	127	0 (1983)	8 (1988)	3.098	1.998	0.031 (0.245)
Other	7873	160 (2014)	239 (1992)	192.024	16.590	**−0.610 (0.004)**

pressure (reduction to sea level using the eta model reduction; NARR variable name "MSLET") was adapted in place of sea surface height. First, local minima in MSLET were identified across the NARR domain. A radius search for each identified minima were then compared with the positions of minima in the previous time step to identify tracks across time. A storm track that no longer identified a closest connecting minimum in surface pressure was assumed to have dissipated. To identify longer lived ETCs with a westerly component to the track, and without any spurious jumps, a set of criteria were implemented. The storm tracking criteria used in this study is an expanded version of the method originally used by Klotzbach et al. (2016). The filter criteria that were applied required that ETCs have (i) a duration of at least 24 h; (ii) a total track distance over 500 km; and, to eliminate meandering systems caused by semipermanent atmospheric circulations, (iii) a ratio between the start-to-end distance over the total track distance greater than 0.6. To perform a complete statistical climatology of ETC frequency and intensity, each ETC's geographical location and minimum mean sea level pressure are recorded from genesis to termination at three-hourly intervals as permitted by NARR. Note that some studies have mentioned concerns with employing mean sea level pressure as the primary tracking variable, citing issues such as being influenced by both large-scale and strong background flow (Hoskins and Hodges 2002; Anderson et al. 2003; Hodges et al. 2003; Wang et al. 2006). However, as noted in Wang et al. (2006), the background flow biases toward slower meandering systems, which are removed from the analysis via the aforementioned criteria.

Some limiting considerations of this tracking algorithm include the sole use of MSLP as the tracked variable. While the algorithm and subsequently applied filtering criterion successfully counted and tracked ETCs, some errors were noted. In one extreme case, Hurricane Wilma (2005) was mistakenly tracked as a 350+-h extratropical cyclone from its genesis point in the Caribbean Sea to its termination in the North Atlantic. An additional limitation to this study is the excluded buffer region from the defined analysis window (Fig. 1), and the full domain of NARR that was placed to prevent cyclones that formed outside the NARR domain, then tracked into it from being counted as cyclogenesis. It is possible that this exclusion could have prevented some cyclones that formed on the fringes of the NARR domain from being counted.

c. *Cyclone classification*

ETC genesis can occur anywhere outside the tropics but has preference for specific geographic regions (e.g., lee of mountains

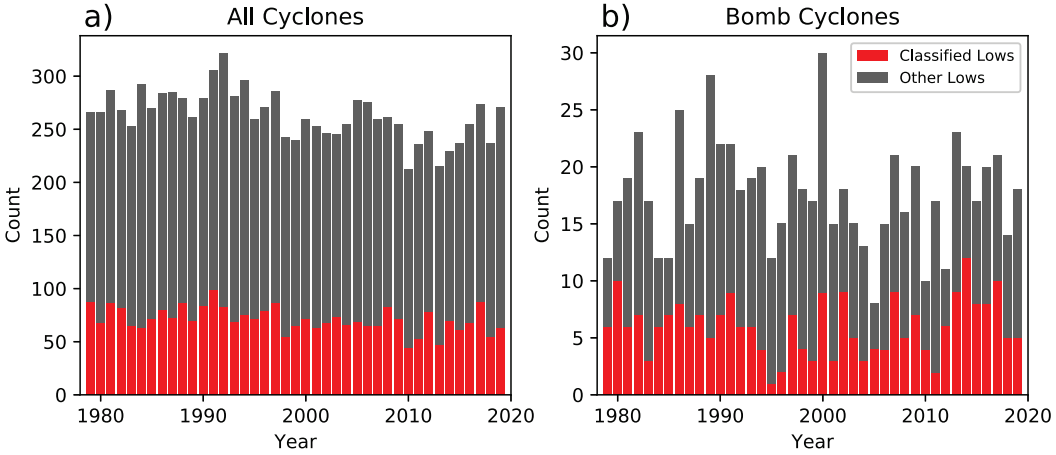

FIG. 3. Annual counts of classified (red) and unclassified (gray) cyclones for (a) any cyclone and (b) bomb cyclones for the period 1979–2019.

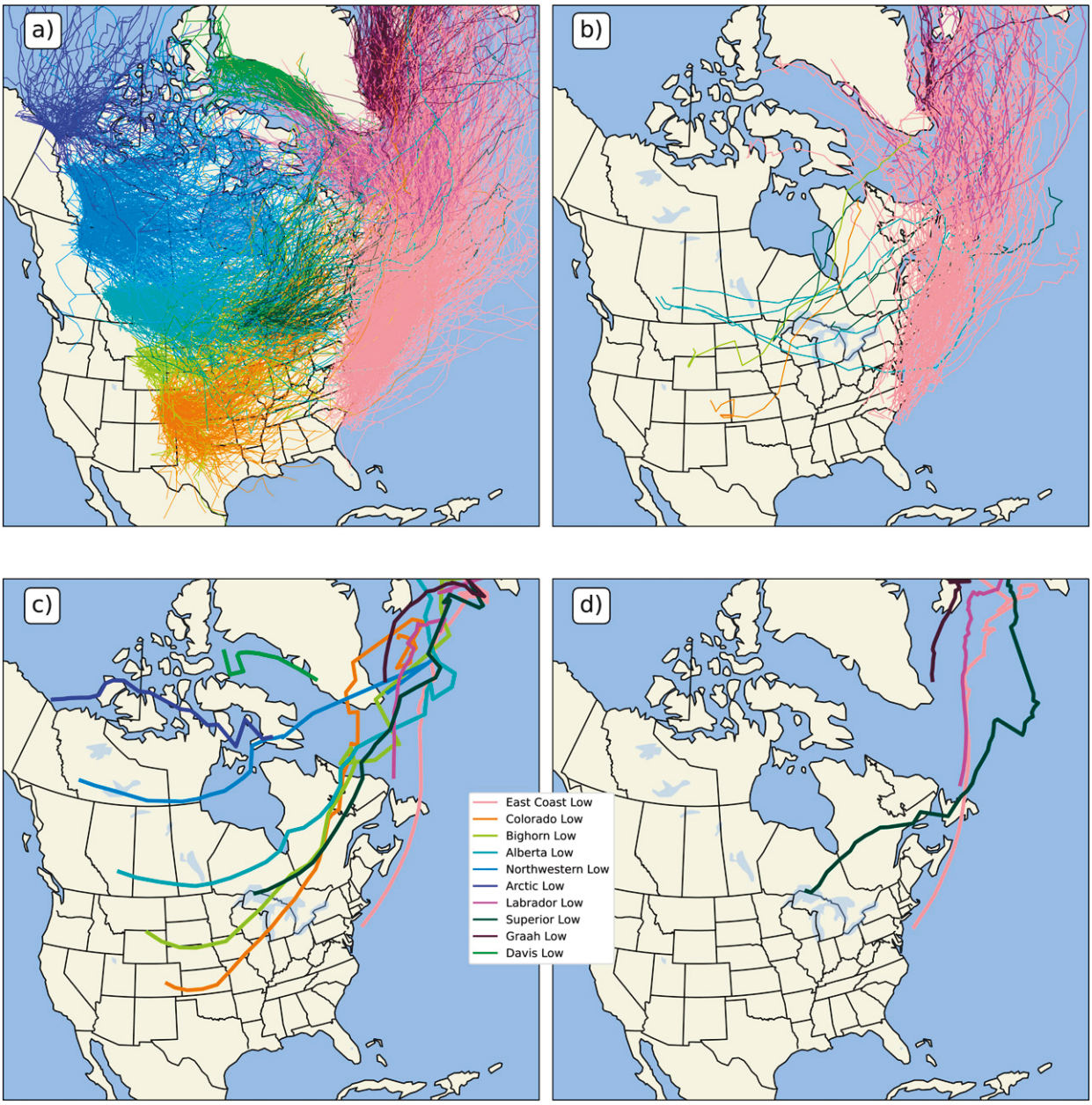

FIG. 4. The 1979–2019 tracks by classification region for (a) all cyclones, (b) bomb cyclones, (c) mean cyclones, and (d) mean bomb cyclones. Mean tracks are only shown for each region if $N \geq 5$.

and continental coastlines). Previous studies identify these areas of high concentration and frequency of cyclogenesis by analyzing horizontal distributions of mean sea level pressure passing through a set of grid points through time (Reitan 1974; Zishka and Smith 1980; Whittaker and Horn 1981; Bannon 1992). To verify these high-concentration cyclogenesis areas set forth by previous studies, an objectively based classification scheme was developed to determine regions of enhanced cyclogenesis. Cyclogenesis counts were aggregated on an equal-area grid and then smoothed by calculating the mean of each grid box and adjacent grid boxes. A threshold value mask of 7 was selected to identify distinct local maxima. A convex hull algorithm was then applied to the thresholded grids and then hand trimmed such that only areas inside the original threshold limit were considered. Following this process, 10 distinct cyclogenesis zones were defined (Fig. 1). While some overlap was found with previous studies such as Whittaker and Horn (1981), the objective classification scheme illustrates a shift in some regions (such as Alberta, Northwest, and East Coast lows), while other historical cyclogenesis areas (such as the Gulf of Mexico and the Great Basin) are no longer favoring continued cyclogenesis. By

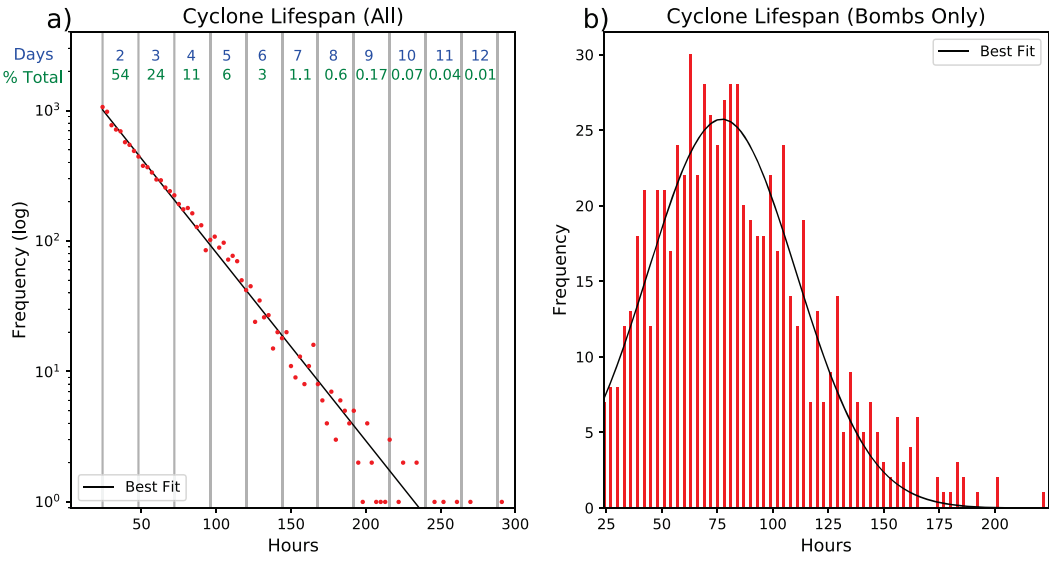

FIG. 5. The life span of (a) all cyclones (N = 10 798) and (b) bomb cyclones (N = 725) tracked in this study. Blue numbers and gray lines in (a) signify days since cyclogenesis. Green numbers indicate the percent total of all cyclones by day.

classifying ETCs, these data can then be stratified by genesis location so that meaningful trends in ETC characterization such as lowest pressure, pressure falls, storm tracks, and frequency may be better observed.

For a cyclone to be classified, the point of genesis needed to fall within the defined region, and the point of termination needed to lie outside the defined region. Any cyclone that did not meet this criterion or formed outside a defined region was

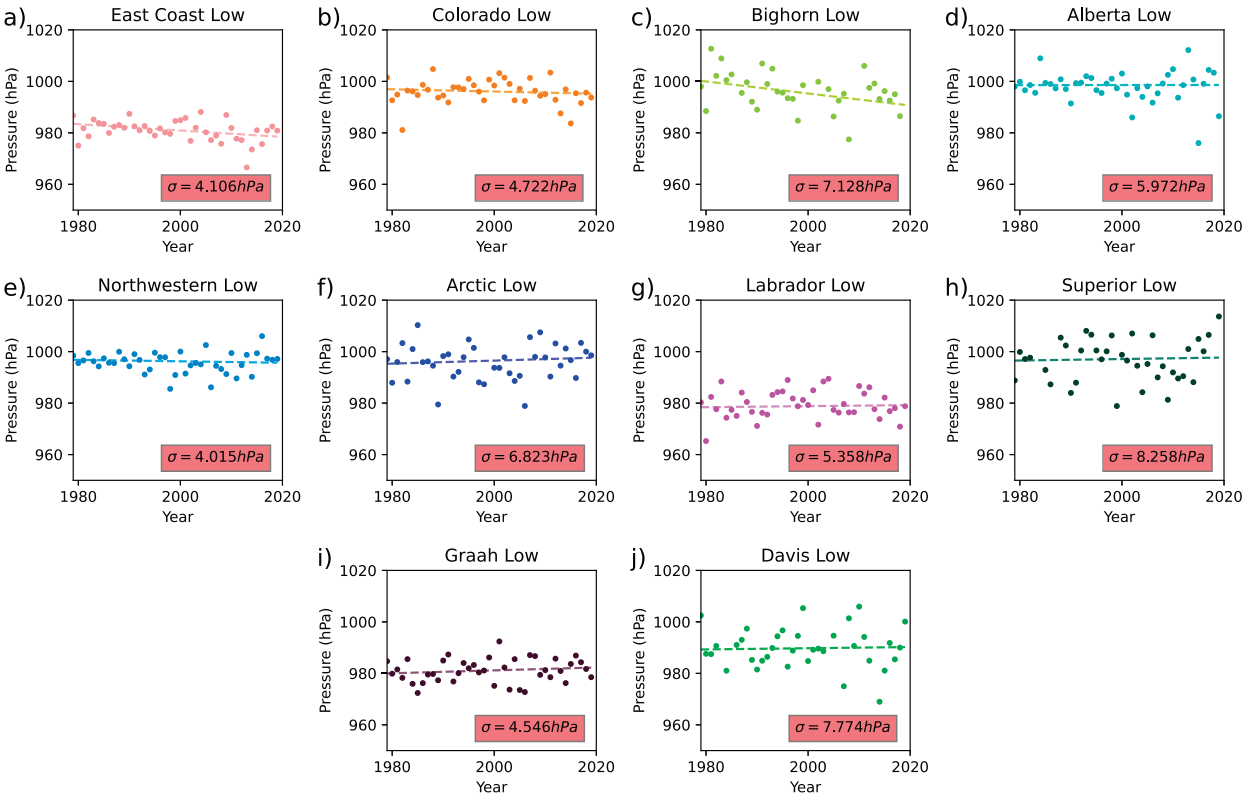

FIG. 6. Annual average of lowest cyclone pressure by classification region. Dashed lines denote the Theil–Sen's linear regression estimator for the points. Standard deviation values of annual average lowest pressure for each classification are also shown.

classified as "other." Explosive ETCs (i.e., bomb cyclones) were classified using the definition of the Bergeron unit (Sanders and Gyakum 1980; Roebber 1984; Gyakum et al. 1989; Chen et al. 1992). For each ETC, a Bergeron unit was calculated for each rolling 3-h time step by analyzing the previous 24-h MSLET values. If the Bergeron value exceeded 1 at any interval, the cyclone was classified as a bomb cyclone and the cyclogenesis location was noted.

3. Results

a. *Spatial frequency and variability of extratropical cyclones*

Interannual (1979–2019) frequencies of cool-season (October–April) ETCs were tallied across North America and segmented by genesis region (Fig. 2a). In total, the algorithm counted 10 671 ETCs in the identified regions during the 40-yr study period. Year-to-year variability of the total summed frequency of ETCs from this study's defined regions is noticeable, with counts ranging from 44 to 99 per year. Genesis regions responsible for the highest ETC counts are East Coast lows ($N = 741$), northwestern lows ($N = 500$), and Labrador lows ($N = 385$) because of the relatively larger geographical size of each region (Table 1). To alleviate the regional domain size disparities, ETC frequencies were normalized by area and calculated as a percent of the total ETC counts for the year (Fig. 2c). When normalized by area, Colorado lows (25.39%) are generally the most numerous each year, followed by Alberta lows (17.76%) and East Coast lows (14.30%).

Summary statistics of cyclone frequencies for each classification were calculated (Table 1). Alberta, Arctic, Bighorn, Davis, East Coast, Labrador, and Superior lows have not seen any statistically significant (linear regression p value < 0.05) changes in frequency over the 40-yr window, whereas Colorado, Graah, and Northwest lows have all demonstrated statistically significant decreasing trends in ETC frequency. These, in addition to lows classified as other, which account for a majority of ETCs across North America (Table 1; Fig. 3a), have shown statistically significant decreasing trends, in agreement with previous studies (Sickmöller et al. 2000; Gulev et al. 2001; McCabe et al. 2001; Wang et al. 2006; Raible et al. 2008; Ulbrich et al. 2009). When considering all cyclones (classified and nonclassified), a statistically significant decrease (−1.045 cyclones per year; $p = 0.000\,229$) using linear regression was found.

Bomb cyclone counts also show interannual variability ranging from 8 to 30 per year across the analysis domain (Fig. 3b). On average, the East Coast region sees at least one bomb cyclone per year (with a maximum frequency of eight in 1980), with other regions registering one bomb cyclone every few years (Fig. 2b). It is important to note that a large number of bomb cyclones did occur outside the defined classification zones (Fig. 3b).

b. *Extratropical cyclone tracks*

Cool-season ETC tracks were also examined over the 40-yr analysis period and study domain. Classified genesis zones of ETCs affect most regions to the east of the Rockies of North America (Fig. 4a), with the highest concentration of tracks clustering east of the Alberta Rocky Mountain foothills, east of the Colorado Rocky Mountain foothills, east of the Rocky Mountain foothills in the Northwest Territories, along the U.S. East Coast, in the Labrador Sea, and east of the Graah Mountain Range (Figs. 4a, 8a,b).

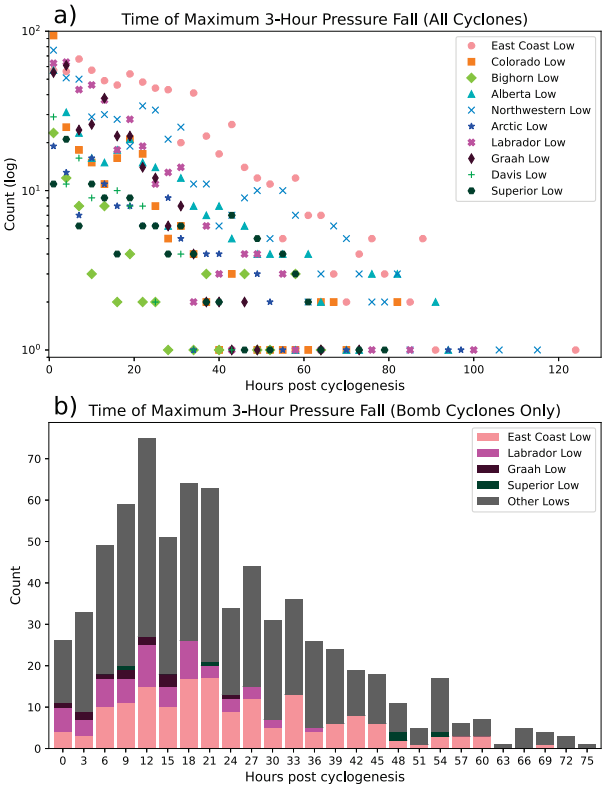

FIG. 7. Frequency analysis of the 3-h time step with greatest pressure fall for (a) all regionally classified cyclones and (b) bomb cyclones.

The mean track for all ETCs in the dataset for each of the regional classification zones were determined (Fig. 4c). Mean tracks for regional classifications show a consistent eastward and poleward track after genesis, with the exception of Davis lows, which track westward and poleward. The greatest variability over the lifetime of the track occurs with Colorado lows, which exhibit a standard deviation in the mean latitude of 9.1°, followed by Bighorn lows with a standard deviation of 6.3°. The lowest variability in the mean track latitude occurs with Northwest lows with a standard deviations of 1.8°.

A majority of all classified bomb cyclones for this study were East Coast lows (Fig. 4b). Most classification regions either do not have a recorded bomb cyclone, or only have a very limited number of classified bomb cyclones (e.g., $N < 5$). The mean tracks of bomb cyclones are presented for all classifications that had at least five recorded bomb cyclones (Fig. 4d). Overall mean bomb tracks are consistent with mean tracks of all cyclones in each region, tending to rapidly move poleward after genesis, with the exception of Superior lows, which tend to

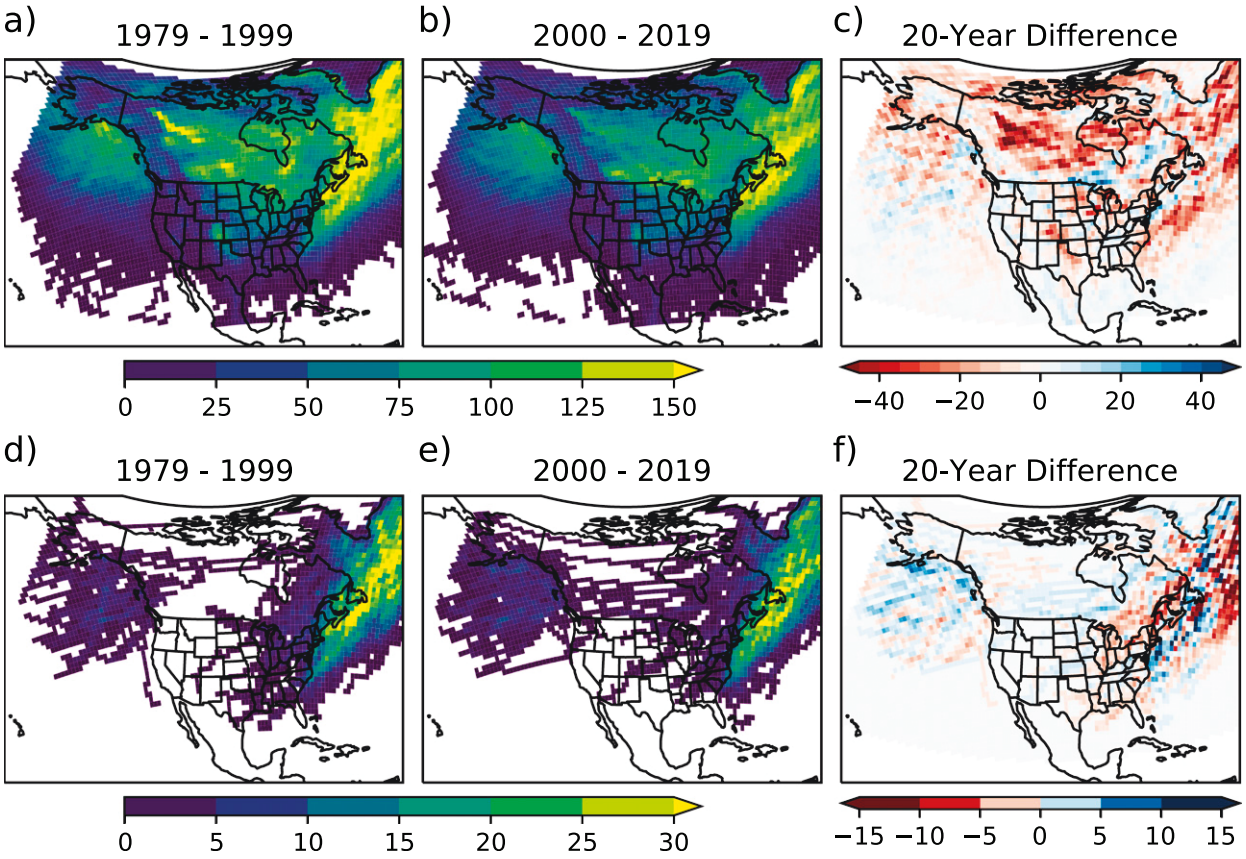

FIG. 8. Equal-area grid counts of (a)–(c) all cyclone tracks and (d)–(f) only bomb cyclone tracks for (left) 1979–99 and (center) 2000–19, with (right) the difference between epochs.

have a more zonal component until they reach the Atlantic Ocean, then rapidly translate poleward.

c. *Life span and intensification*

In general, a log-linear relationship was noted between ETC life span and frequency (Fig. 5a), whereas bomb cyclones display a distinct peak life span of approximately 75 h (Fig. 5b). The lowest pressure for each ETC track was recorded in an effort to tally the annual average of the minimum ETC pressure by each genesis region (Fig. 6). This was performed to understand if there have been any significant trends in minimum ETC pressure through time. When examining the annual average of these lowest mean sea level central pressure values, most genesis regions displayed a slight negative trend toward lower pressure (i.e., stronger cyclones). However, only the East Coast (Fig. 6a) and Bighorn ETCs (Fig. 6c) slopes were significant at the 95% confidence level when analyzing Theil–Sen's slope and Kendall's τ statistic. Superior ETCs (Fig. 6h) exhibited the greatest standard deviation in interannual average lowest pressure (8.258 hPa), while Northwest lows (Fig. 6) exhibited the lowest standard deviation in average lowest cyclone pressure (4.015 hPa).

In addition to the lowest pressure along the ETC track, the time of maximum 3-h pressure fall was calculated and plotted as a frequency relative to time after ETC genesis (Fig. 7a). This was also performed for bomb ETCs (Fig. 7b). Log-linear relationships were again noted for all cyclones, as 88% of all cyclones experience their maximum 3-h pressure fall value by 42 h postgenesis (Fig. 7a). Maximum 3-h pressure fall value in bomb cyclone tracks—especially in the classified regions—displayed a more consistent distribution across a broad range of postgenesis temporal epochs (e.g., similar frequencies at 12 and 27 h after cyclogenesis). Maximum 3-h pressure falls for East Coast low bomb cyclones display two peaks near 18–21 h after genesis and 33–36 h after genesis, with peaks for all classified lows occurring at 12–14 h and 20–24 h after genesis (Fig. 7b).

d. *Trends in spatial frequency*

Gridded analysis of all ETC tracks over the analysis domain and temporal period are presented in Fig. 8 using equal-area grid boxes to address the sensitivity of latitude projections in spatial count analysis (Hayden 1981). Counts of ETC tracks between 1979 and 1999 (Fig. 8a) and 2000 and 2019 (Fig. 8b), and the difference between these 20-yr epochs (Fig. 8c) display a clear signal of decreasing ETC trends across expansive regions in the Northern Hemisphere, which is in agreement with various aspects from previous research (e.g., Sickmöller et al. 2000; Gulev et al. 2001; McCabe et al. 2001; Wang et al. 2006; Raible et al. 2008; Ulbrich et al. 2009).

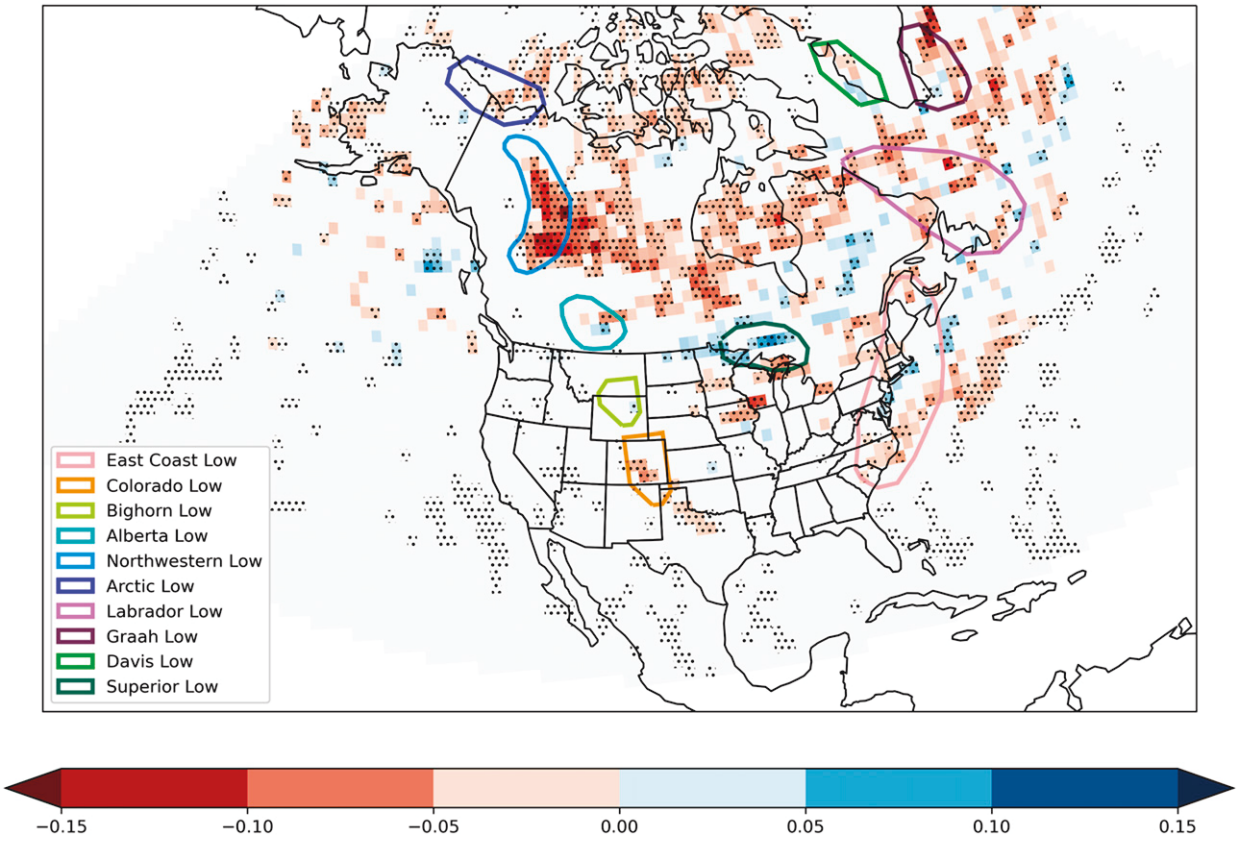

FIG. 9. Equal-area gridpoint trends (counts per year) of cyclone counts for 1979–2019 using Theil–Sen's slope. Stippled values indicate a statistically significant trend at the 95% confidence level using Kendall's τ statistic.

By using 20-yr intervals, large scale teleconnection influences on cyclone frequency are reduced. To assess statistical significance in these gridpoint changes, Theil–Sen's slope (Theil 1950; Sen 1960) was calculated on each grid box for each year's ETC track counts and overlaid with Kendall's τ statistic to determine statistical significance (Fig. 9). Theil–Sen's slope is a more robust trend estimator for temporal data as it is insensitive to outliers and can be more accurate than simple linear regression for nonhomogeneous or skewed data. Analysis of Theil–Sen's slope for ETC track counts show a region of statistically significant decrease occurring in central Canada, mainly to the east of the Alberta Rocky Mountain Range, into central Saskatchewan, Manitoba, and northern Ontario along the Hudson Bay. A notable zone of statistically significant ETC track decrease was also found along central Iowa and southern Wisconsin. The difference of total ETC counts were again applied to the monthly totals of October–April using the same epochs of 1979–99 and 2000–19 (Fig. 10). A clear majority of cyclone track counts across the cool-season months have shown a decreasing trend, although some regional increases are noted, such as the Lake Superior region in February (Fig. 10e).

Gridded analysis for bomb cyclone track frequency was also performed between 1979 and 1999 (Fig. 8d), 2000 and 2019 (Fig. 8e), and the difference between the 20-yr periods (Fig. 8f). Unlike nonexplosive ETCs, bomb cyclone trends do not appear to have any spatial patterns of increasing or decreasing trends, likely due to the large interannual variability in the counts of these cyclones (Fig. 2b). Theil–Sen's slope and Kendall's τ statistic were also calculated for bomb cyclones alone; however, no statistically significant trends were noted across North America.

4. Discussion

The overarching findings of this research conclude a decline in frequency of ETCs across North America, which has been corroborated by other studies (Reitan 1974; Whittaker and Horn 1981; Carnell and Senior 1998; Sickmöller et al. 2000; Gulev et al. 2001; McCabe et al. 2001; Bengtsson et al. 2006; Wang et al. 2006; Raible et al. 2008; Ulbrich et al. 2009). The findings of Whittaker and Horn (1981), which looked at cyclone frequency from 1958 to 1977, closely resemble the findings of this study with a statistically significant decrease in high-latitude ETC and limited statistical trends in CONUS ETC frequency. Thiel–Sen's slope and Kendall's τ statistic indicated a large swath across central Canada undergoing a statistically significant decrease in ETC track frequency. Decreases appear to be occurring across the entire cold season, with all months of the analysis (October–April) illustrating at least some level of decrease across central Canada (Fig. 10). The small region to the

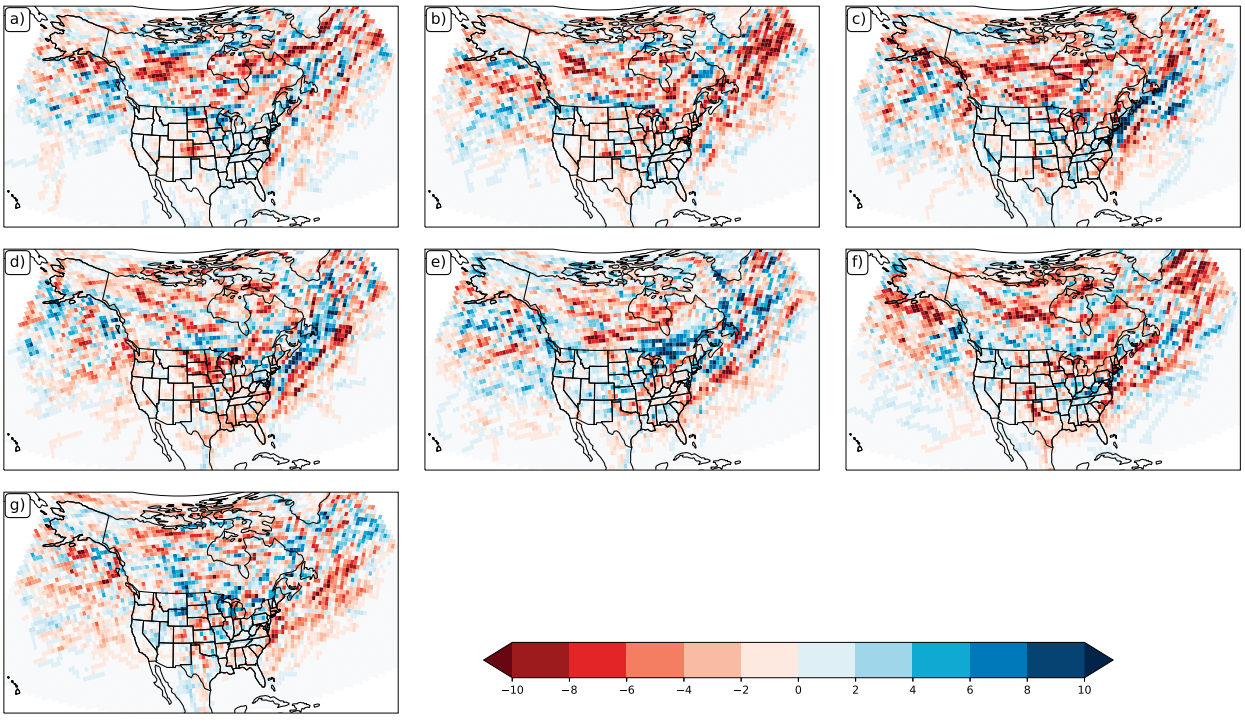

FIG. 10. Equal-area grid count differences (1979–99 minus 2000–19) of all cyclone tracks for (a) October, (b) November, (c) December, (d) January, (e) February, (f) March, and (g) April.

north of Lake Superior displays a statistically significant increase in ETC frequency over the analysis window, with largest increase in frequency during the months of April, October, and December. Two possible explanations for this region's increase in frequency, noted originally by Reitan (1974), could be an intersection of the Colorado, Bighorn, and Alberta low tracks alongside a region of enhanced localized cyclogenesis caused by the relatively warm lake waters in the winter months acting as a diabatic heat source and aiding cyclogenesis (Danard and Mcmillan 1974; Sousounis and Fritsch 1994; Scott and Huff 1996).

When analyzing ETC track frequency (Fig. 8), a decrease in nonexplosive East Coast lows was found to have occurred; however, no statistically significant increase in bomb cyclones was determined to be present for the same location. In addition, the Bay of Alaska and East Coast (Fig. 8f) were determined to be locales of increasing bomb cyclone occurrence. One study analyzed the trends in developing extreme cyclones, defined as a cyclone whose strength was in the top 10% of all cyclones, and found a net decrease in extreme cyclones in the Northern Hemisphere (Pinto et al. 2009). The findings of Pinto et al. (2009) concluded that no statistical trends in extreme cyclone frequency were present, a result that this study similarly determined with interannual bomb cyclone frequency.

Previous studies have considered the decrease in ETC counts for North America to be due to a poleward shift in the overall storm track as a response to climate change (Yin 2005; Bender et al. 2012; Vose et al. 2014; Tamarin and Kaspi 2017), supporting a decrease in midlatitude cyclones and an increase in high-latitude cyclones (McCabe et al. 2001; Karl et al. 2009; Vose et al. 2014). This study contradicts these findings, noting that a decline of both mid- and higher-latitude cyclones having occurred over the past 40-yr, at least in the NARR domain (Fig. 8c). The frequency of Colorado, Graah, and Northwestern lows have decreased the with greatest statistical significance (Table 1; Fig. 9).

Study findings identify that 89% of all ETCs have a 2–4-day life span (Fig. 5a), which is similar to findings in previous literature that also determined the mean life span for North American ETCs to be 2–4 days (Gulev et al. 2001). Approximately 0.89% of all ETCs tracked in this study lasted over 8 days, contradicting findings from Gulev et al. (2001) that found 21% of North American continental cyclones have a life span over 8 days. This difference may be due a coarser dataset used (6-hourly NCEP–NCAR SLP fields and 2.5° × 2.5° grid) or to the limited eastward extent of the NARR domain for life-span tracking. Most bomb cyclones show a life span of 62–80 h as compared with previous research citing 72–144 h for Northern Hemisphere bomb cyclones (Reale et al. 2019). One outlying bomb cyclone event is noted with a life span of 350 h and is determined to be 2005's Hurricane Wilma. As tropical cyclones move into midlatitudes, a large number undergo transition into ETCs (Hart and Evans 2001; Jones et al. 2003).

5. Conclusions

This study used reanalysis mean sea level pressure at ~32-km horizontal grid spacing with 3-h intervals to determine trends of

cool-season (October–April) ETCs in North America from 1979 to 2019. ETCs were tracked using a modified eddy tracking algorithm (Chelton et al. 2011), subject to a set of filter criterion for defining an ETC (Klotzbach et al. 2016). ETCs were classified by regions of cyclogenesis counted on an equal-area grid, and bomb cyclones were classified using the definition of the Bergeron unit (Sanders and Gyakum 1980; Roebber 1984; Gyakum et al. 1989; Chen et al. 1992).

This study's findings generally agree with previous literature citing an overall decreasing trend in ETC frequency over North America (Sickmöller et al. 2000; Gulev et al. 2001; McCabe et al. 2001; Wang et al. 2006; Raible et al. 2008; Ulbrich et al. 2009). In particular, this study determined that ETC genesis in Colorado, Graah, and the Northwest has undergone statistically significant decreases in the last 40 years. A gridded equal-area Theil–Sen's slope analysis of storm tracks over the analysis window reveals a statistically significant reduction in ETC frequency across Canada's Northwest Territories, and this decrease was most notable in March (although all months demonstrate a varying degree of decline in frequency). A small region north of Lake Superior, along the U.S.-Canada border, illustrated an increasing trend in ETC track counts. An examination of ETC frequency and life span shows a log-linear relationship. In addition, a statistically significant negative trend in ETC minimum pressure was observed with East Coast lows, and 88% of all ETCs experience their maximum 3-h pressure fall within the first 42 h after cyclogenesis. Results from this study provide important statistics about ETC frequency and location, as well as their recent trends. Future work should continue to monitor and further assess the causal mechanisms of these trends.

Acknowledgments. Three anonymous reviewers provided suggestions that greatly improved this paper. This research was partially funded by a Northern Illinois University Research and Artistry award and by the National Science Foundation (Award 2048770).

REFERENCES

Allen, J. T., A. B. Pezza, and M. T. Black, 2010: Explosive cyclogenesis: A global climatology comparing multiple reanalyses. *J. Climate*, **23**, 6468–6484, https://doi.org/10.1175/2010JCLI3437.1.

Alpert, P., B. U. Neeman, and Y. Shay-El, 1990: Climatological analysis of Mediterranean cyclones using ECMWF data. *Tellus*, **42A**, 65–77, https://doi.org/10.3402/tellusa.v42i1.11860.

Anderson, D., K. I. Hodges, and B. J. Hoskins, 2003: Sensitivity of feature-based analysis methods of storm tracks to the form of background field removal. *Mon. Wea. Rev.*, **131**, 565–573, https://doi.org/10.1175/1520-0493(2003)131<0565:SOFBAM>2.0.CO;2.

Attard, H. E., and A. L. Lang, 2019: The impact of tropospheric and stratospheric tropical variability on the location, frequency, and duration of cool-season extratropical synoptic events. *Mon. Wea. Rev.*, **147**, 519–542, https://doi.org/10.1175/MWR-D-18-0039.1.

Bannon, P. R., 1992: A model of Rocky Mountain lee cyclogenesis. *J. Atmos. Sci.*, **49**, 1510–1522, https://doi.org/10.1175/1520-0469(1992)049<1510:AMORML>2.0.CO;2.

Befort, D. J., S. Wild, T. Kruschke, U. Ulbrich, and G. C. Leckebusch, 2016: Different long-term trends of extra-tropical cyclones and windstorms in ERA-20C and NOAA-20CR reanalyses. *Atmos. Sci. Lett.*, **17**, 586–595, https://doi.org/10.1002/asl.694.

Bender, F. A., V. Ramanathan, and G. Tselioudis, 2012: Changes in extratropical storm track cloudiness 1983–2008: Observational support for a poleward shift. *Climate Dyn.*, **38**, 2037–2053, https://doi.org/10.1007/s00382-011-1065-6.

Bengtsson, L., K. I. Hodges, and E. Roeckner, 2006: Storm tracks and climate change. *J. Climate*, **19**, 3518–3543, https://doi.org/10.1175/JCLI3815.1.

Bentley, A. M., L. F. Bosart, and D. Keyser, 2019: A climatology of extratropical cyclones leading to extreme weather events over central and eastern North America. *Mon. Wea. Rev.*, **147**, 1471–1490, https://doi.org/10.1175/MWR-D-18-0453.1.

Bernhardt, J. E., and A. T. DeGaetano, 2012: Meteorological factors affecting the speed of movement and related impacts of extratropical cyclones along the US East Coast. *Nat. Hazards*, **61**, 1463–1472, https://doi.org/10.1007/s11069-011-0078-0.

Blender, R., and M. Schubert, 2000: Cyclone tracking in different spatial and temporal resolutions. *Mon. Wea. Rev.*, **128**, 377–384, https://doi.org/10.1175/1520-0493(2000)128<0377:CTIDSA>2.0.CO;2.

Bullock, T. A., and J. R. Gyakum, 1993: A diagnostic study of cyclogenesis in the western North Pacific Ocean. *Mon. Wea. Rev.*, **121**, 65–75, https://doi.org/10.1175/1520-0493(1993)121<0065:ADSOCI>2.0.CO;2.

Carnell, R., and C. Senior, 1998: Changes in mid-latitude variability due to increasing greenhouse gases and sulphate aerosols. *Climate Dyn.*, **14**, 369–383, https://doi.org/10.1007/s003820050229.

Chang, E. K., S. Lee, and K. L. Swanson, 2002: Storm track dynamics. *J. Climate*, **15**, 2163–2183, https://doi.org/10.1175/1520-0442(2002)015<02163:STD>2.0.CO;2.

Changnon, D., J. J. Noel, and L. H. Maze, 1995: Determining cyclone frequencies using equal-area circles. *Mon. Wea. Rev.*, **123**, 2285–2294, https://doi.org/10.1175/1520-0493(1995)123<2285:DCFUEA>2.0.CO;2.

Chelton, D. B., M. G. Schlax, and R. M. Samelson, 2011: Global observations of nonlinear mesoscale eddies. *Prog. Oceanogr.*, **91**, 167–216, https://doi.org/10.1016/j.pocean.2011.01.002.

Chen, S.-J., Y.-H. Kuo, P.-Z. Zhang, and Q.-F. Bai, 1992: Climatology of explosive cyclones off the East Asian coast. *Mon. Wea. Rev.*, **120**, 3029–3035, https://doi.org/10.1175/1520-0493(1992)120<3029:COECOT>2.0.CO;2.

Chung, Y.-S., and E. R. Reinelt, 1973: On cyclogenesis in the lee of the Canadian Rocky Mountains. *Arch. Meteor. Geophys. Bioklimatol.*, **22A**, 205–226, https://doi.org/10.1007/BF02247545.

——, K. D. Hage, and E. R. Reinelt, 1976: On lee cyclogenesis and airflow in the Canadian Rocky Mountains and the East Asian mountains. *Mon. Wea. Rev.*, **104**, 879–891, https://doi.org/10.1175/1520-0493(1976)104<0879:OLCAAI>2.0.CO;2.

Colle, B. A., J. F. Booth, and E. K. Chang, 2015: A review of historical and future changes of extratropical cyclones and associated impacts along the US East Coast. *Curr. Climate Change Rep.*, **1**, 125–143, https://doi.org/10.1007/s40641-015-0013-7.

Danard, M. B., and A. C. Mcmillan, 1974: Further numerical studies of the effects of the Great Lakes on winter cyclones. *Mon. Wea. Rev.*, **102**, 166–175, https://doi.org/10.1175/1520-0493(1974)102<0166:FNSOTE>2.0.CO;2.

Eichler, T., and W. Higgins, 2006: Climatology and ENSO-related variability of North American extratropical cyclone activity. *J. Climate*, **19**, 2076–2093, https://doi.org/10.1175/JCLI3725.1.

Fink, A. H., T. Brücher, V. Ermert, A. Krüger, and J. G. Pinto, 2009: The European storm Kyrill in January 2007: Synoptic

evolution, meteorological impacts and some considerations with respect to climate change. *Nat. Hazards Earth Syst. Sci.*, **9**, 405–423, https://doi.org/10.5194/nhess-9-405-2009.

Grise, K. M., S.-W. Son, and J. R. Gyakum, 2013: Intraseasonal and interannual variability in North American storm tracks and its relationship to equatorial Pacific variability. *Mon. Wea. Rev.*, **141**, 3610–3625, https://doi.org/10.1175/MWR-D-12-00322.1.

Gulev, S., O. Zolina, and S. Grigoriev, 2001: Extratropical cyclone variability in the Northern Hemisphere winter from the NCEP/NCAR reanalysis data. *Climate Dyn.*, **17**, 795–809, https://doi.org/10.1007/s003820000145.

Gyakum, J. R., and R. E. Danielson, 2000: Analysis of meteorological precursors to ordinary and explosive cyclogenesis in the western North Pacific. *Mon. Wea. Rev.*, **128**, 851–863, https://doi.org/10.1175/1520-0493(2000)128<0851:AOMPTO>2.0.CO;2.

——, J. R. Anderson, R. H. Grumm, and E. L. Gruner, 1989: North Pacific cold-season surface cyclone activity: 1975–1983. *Mon. Wea. Rev.*, **117**, 1141–1155, https://doi.org/10.1175/1520-0493(1989)117<1141:NPCSSC>2.0.CO;2.

Hart, R. E., and J. L. Evans, 2001: A climatology of the extratropical transition of Atlantic tropical cyclones. *J. Climate*, **14**, 546–564, https://doi.org/10.1175/1520-0442(2001)014<0546:ACOTET>2.0.CO;2.

Hayden, B. P., 1981: Cyclone occurrence mapping: Equal area or raw frequencies? *Mon. Wea. Rev.*, **109**, 168–172, https://doi.org/10.1175/1520-0493(1981)109<0168:COMEAO>2.0.CO;2.

Hirsch, M. E., A. T. DeGaetano, and S. J. Colucci, 2001: An East Coast winter storm climatology. *J. Climate*, **14**, 882–899, https://doi.org/10.1175/1520-0442(2001)014<0882:AECWSC>2.0.CO;2.

Hodges, K. I., 1994: A general method for tracking analysis and its application to meteorological data. *Mon. Wea. Rev.*, **122**, 2573–2586, https://doi.org/10.1175/1520-0493(1994)122<2573:AGMFTA>2.0.CO;2.

——, 1996: Spherical nonparametric estimators applied to the UGAMP model integration for AMIP. *Mon. Wea. Rev.*, **124**, 2914–2932, https://doi.org/10.1175/1520-0493(1996)124<2914:SNEATT>2.0.CO;2.

——, B. J. Hoskins, J. Boyle, and C. Thorncroft, 2003: A comparison of recent reanalysis datasets using objective feature tracking: Storm tracks and tropical easterly waves. *Mon. Wea. Rev.*, **131**, 2012–2037, https://doi.org/10.1175/1520-0493(2003)131<2012:ACORRD>2.0.CO;2.

Holton, J. R., 2004: *An Introduction to Dynamic Meteorology*. 4th ed. Elsevier, 552 pp.

Hoskins, B. J., and K. I. Hodges, 2002: New perspectives on the Northern Hemisphere winter storm tracks. *J. Atmos. Sci.*, **59**, 1041–1061, https://doi.org/10.1175/1520-0469(2002)059<1041:NPOTNH>2.0.CO;2.

Jones, S. C., and Coauthors, 2003: The extratropical transition of tropical cyclones: Forecast challenges, current understanding, and future directions. *Wea. Forecasting*, **18**, 1052–1092, https://doi.org/10.1175/1520-0434(2003)018<1052:TETOTC>2.0.CO;2.

Karl, T. R., J. M. Melillo, T. C. Peterson, and S. J. Hassol, 2009: *Global Climate Change Impacts in the United States*. Cambridge University Press, 189 pp.

Klotzbach, P. J., E. C. Oliver, R. D. Leeper, and C. J. Schreck III, 2016: The relationship between the Madden–Julian oscillation (MJO) and southeastern New England snowfall. *Mon. Wea. Rev.*, **144**, 1355–1362, https://doi.org/10.1175/MWR-D-15-0434.1.

König, W., R. Sausen, and F. Sielmann, 1993: Objective identification of cyclones in GCM simulations. *J. Climate*, **6**, 2217–2231, https://doi.org/10.1175/1520-0442(1993)006<2217:OIOCIG>2.0.CO;2.

Lackmann, G., 2011: *Midlatitude Synoptic Meteorology: Dynamics, Analysis, and Forecasting*. Amer. Meteor. Soc., 345 pp.

Lamb, P. J., and S. A. Changnon Jr., 1981: On the "best" temperature and precipitation normals: The Illinois situation. *J. Appl. Meteor.*, **20**, 1383–1390, https://doi.org/10.1175/1520-0450(1981)020<1383:OTTAPN>2.0.CO;2.

Le Treut, H., and E. Kalnay, 1990: Comparison of observed and simulated cyclone frequency distribution as determined by an objective method. *Atmósfera*, **3**, 57–71.

Martin, J. E., 2013: *Mid-Latitude Atmospheric Dynamics: A First Course*. John Wiley and Sons, 336 pp.

McCabe, G. J., M. P. Clark, and M. C. Serreze, 2001: Trends in Northern Hemisphere surface cyclone frequency and intensity. *J. Climate*, **14**, 2763–2768, https://doi.org/10.1175/1520-0442(2001)014<2763:TINHSC>2.0.CO;2.

McDonald, R. E., 2011: Understanding the impact of climate change on Northern Hemisphere extra-tropical cyclones. *Climate Dyn.*, **37**, 1399–1425, https://doi.org/10.1007/s00382-010-0916-x.

Mesinger, F., and Coauthors, 2006: North American Regional Reanalysis. *Bull. Amer. Meteor. Soc.*, **87**, 343–360, https://doi.org/10.1175/BAMS-87-3-343.

Murray, R. J., and I. Simmonds, 1991: A numerical scheme for tracking cyclone centres from digital data. Part II: Application to January and July general circulation model simulations. *Aust. Meteor. Mag.*, **39**, 167–180.

Pinto, J. G., S. Zacharias, A. H. Fink, G. C. Leckebusch, and U. Ulbrich, 2009: Factors contributing to the development of extreme North Atlantic cyclones and their relationship with the NAO. *Climate Dyn.*, **32**, 711–737, https://doi.org/10.1007/s00382-008-0396-4.

Pnevmatikos, J., and B. Katsoulis, 2006: The changing rainfall regime in Greece and its impact on climatological means. *Meteor. Appl.*, **13**, 331–345, https://doi.org/10.1017/S1350482706002350.

Raible, C., P. Della-Marta, C. Schwierz, H. Wernli, and R. Blender, 2008: Northern Hemisphere extratropical cyclones: A comparison of detection and tracking methods and different reanalyses. *Mon. Wea. Rev.*, **136**, 880–897, https://doi.org/10.1175/2007MWR2143.1.

Reale, M., M. L. Liberato, P. Lionello, J. G. Pinto, S. Salon, and S. Ulbrich, 2019: A global climatology of explosive cyclones using a multi-tracking approach. *Tellus*, **71A**, 1611340, https://doi.org/10.1080/16000870.2019.1611340.

Reed, R. J., M. D. Albright, A. J. Sammons, and P. Undén, 1988: The role of latent heat release in explosive cyclogenesis: Three examples based on ECMWF operational forecasts. *Wea. Forecasting*, **3**, 217–229, https://doi.org/10.1175/1520-0434(1988)003<0217:TROLHR>2.0.CO;2.

Reitan, C. H., 1974: Frequencies of cyclones and cyclogenesis for North America, 1951–1970. *Mon. Wea. Rev.*, **102**, 861–868, https://doi.org/10.1175/1520-0493(1974)102<0861:FOCACF>2.0.CO;2.

——, 1979: Trends in the frequencies of cyclone activity over North America. *Mon. Wea. Rev.*, **107**, 1684–1688, https://doi.org/10.1175/1520-0493(1979)107<1684:TITFOC>2.0.CO;2.

Roebber, P. J., 1984: Statistical analysis and updated climatology of explosive cyclones. *Mon. Wea. Rev.*, **112**, 1577–1589, https://doi.org/10.1175/1520-0493(1984)112<1577:SAAUCO>2.0.CO;2.

——, and M. R. Schumann, 2011: Physical processes governing the rapid deepening tail of maritime cyclogenesis. *Mon. Wea. Rev.*, **139**, 2776–2789, https://doi.org/10.1175/MWR-D-10-05002.1.

Salmon, E. M., and P. J. Smith, 1980: A synoptic analysis of the 25–26 January 1978 blizzard cyclone in the central United

States. *Bull. Amer. Meteor. Soc.*, **61**, 453–460, https://doi.org/10.1175/1520-0477(1980)061<0453:FOFASA>2.0.CO;2.

Sanders, F., and J. R. Gyakum, 1980: Synoptic-dynamic climatology of the "bomb." *Mon. Wea. Rev.*, **108**, 1589–1606, https://doi.org/10.1175/1520-0493(1980)108<1589:SDCOT>2.0.CO;2.

Scott, R. W., and F. A. Huff, 1996: Impacts of the Great Lakes on regional climate conditions. *J. Great Lakes Res.*, **22**, 845–863, https://doi.org/10.1016/S0380-1330(96)71006-7.

Sen, P. K., 1960: On some convergence properties of U-statistics. *Calcutta Stat. Assoc. Bull.*, **10** (1–2), 1–18, https://doi.org/10.1177/0008068319600101.

Sickmöller, M., R. Blender, and K. Fraedrich, 2000: Observed winter cyclone tracks in the Northern Hemisphere in re-analysed ECMWF data. *Quart. J. Roy. Meteor. Soc.*, **126**, 591–620, https://doi.org/10.1002/qj.49712656311.

Sinclair, M. R., 1994: An objective cyclone climatology for the Southern Hemisphere. *Mon. Wea. Rev.*, **122**, 2239–2256, https://doi.org/10.1175/1520-0493(1994)122<2239:AOCCFT>2.0.CO;2.

——, and I. G. Watterson, 1999: Objective assessment of extra-tropical weather systems in simulated climates. *J. Climate*, **12**, 3467–3485, https://doi.org/10.1175/1520-0442(1999)012<3467:OAOEWS>2.0.CO;2.

Sousounis, P. J., and J. M. Fritsch, 1994: Lake-aggregate mesoscale disturbances. Part II: A case study of the effects on regional and synoptic-scale weather systems. *Bull. Amer. Meteor. Soc.*, **75**, 1793–1812, https://doi.org/10.1175/1520-0477(1994)075<1793:LAMDPI>2.0.CO;2.

Tamarin, T., and Y. Kaspi, 2017: The poleward shift of storm tracks under global warming: A Lagrangian perspective. *Geophys. Res. Lett.*, **44**, 10 666–10 674, https://doi.org/10.1002/2017GL073633.

Theil, H., 1950: A rank-invariant method of linear and polynomial regression analysis, 3; confidence regions for the parameters of polynomial regression equations. *Indag. Math.*, **1**, 467–482.

Tracton, M. S., 1973: The role of cumulus convection in the development of extratropical cyclones. *Mon. Wea. Rev.*, **101**, 573–593, https://doi.org/10.1175/1520-0493(1973)101<0573:TROCCI>2.3.CO;2.

Uccellini, L. W., P. J. Kocin, R. A. Petersen, C. H. Wash, and K. F. Brill, 1984: The Presidents' Day cyclone of 18–19 February 1979: Synoptic overview and analysis of the subtropical jet streak influencing the pre-cyclogenetic period. *Mon. Wea. Rev.*, **112**, 31–55, https://doi.org/10.1175/1520-0493(1984)112<0031:TPDCOF>2.0.CO;2.

Ulbrich, U., G. Leckebusch, and J. G. Pinto, 2009: Extra-tropical cyclones in the present and future climate: A review. *Theor. Appl. Climatol.*, **96**, 117–131, https://doi.org/10.1007/s00704-008-0083-8.

Vose, R. S., and Coauthors, 2014: Monitoring and understanding changes in extremes: Extratropical storms, winds, and waves. *Bull. Amer. Meteor. Soc.*, **95**, 377–386, https://doi.org/10.1175/BAMS-D-12-00162.1.

Wang, X. L., V. R. Swail, and F. W. Zwiers, 2006: Climatology and changes of extratropical cyclone activity: Comparison of ERA-40 with NCEP–NCAR reanalysis for 1958–2001. *J. Climate*, **19**, 3145–3166, https://doi.org/10.1175/JCLI3781.1.

——, and Coauthors, 2011: Trends and low-frequency variability of storminess over western Europe, 1878–2007. *Climate Dyn.*, **37**, 2355–2371, https://doi.org/10.1007/s00382-011-1107-0.

——, Y. Feng, G. Compo, V. Swail, F. Zwiers, R. Allan, and P. Sardeshmukh, 2013: Trends and low frequency variability of extra-tropical cyclone activity in the ensemble of twentieth century reanalysis. *Climate Dyn.*, **40**, 2775–2800, https://doi.org/10.1007/s00382-012-1450-9.

Whittaker, L. M., and L. H. Horn, 1981: Geographical and seasonal distribution of North American cyclogenesis, 1958–1977. *Mon. Wea. Rev.*, **109**, 2312–2322, https://doi.org/10.1175/1520-0493(1981)109<2312:GASDON>2.0.CO;2.

WMO, 1971: Climatological normals (CLINO) for climate and climate ship stations for the period 1931–1960. WMO/OMM Tech. Doc. 117, 52 pp.

——, 1989: Calculation of monthly and annual 30-year standard normals. WMO Tech. Doc. 341, 11 pp.

Yin, J. H., 2005: A consistent poleward shift of the storm tracks in simulations of 21st century climate. *Geophys. Res. Lett.*, **32**, L18701, https://doi.org/10.1029/2005GL023684.

Yiou, P., and M. Nogaj, 2004: Extreme climatic events and weather regimes over the North Atlantic: When and where? *Geophys. Res. Lett.*, **31**, L07202, https://doi.org/10.1029/2003GL019119.

Zick, S. E., and C. J. Matyas, 2015: Tropical cyclones in the North American Regional Reanalysis: An assessment of spatial biases in location, intensity, and structure. *J. Geophys. Res. Atmos.*, **120**, 1651–1669, https://doi.org/10.1002/2014JD022417.

Zishka, K. M., and P. J. Smith, 1980: The climatology of cyclones and anticyclones over North America and surrounding ocean environs for January and July, 1950–77. *Mon. Wea. Rev.*, **108**, 387–401, https://doi.org/10.1175/1520-0493(1980)108<0387:TCOCAA>2.0.CO;2.

Zolina, O., and S. K. Gulev, 2002: Improving the accuracy of mapping cyclone numbers and frequencies. *Mon. Wea. Rev.*, **130**, 748–759, https://doi.org/10.1175/1520-0493(2002)130<0748:ITAOMC>2.0.CO;2.